

Ceramic Matrix Materials

Materials Manufacturing and Engineering

Edited by
J. Paulo Davim

DE GRUYTER

Editor

Prof. Dr. J. Paulo Davim
University of Aveiro
Department of Mechanical Engineering
Campus Santiago
3810-193 Aveiro, Portugal
pdavim@ua.pt

ISBN 978-3-11-029222-0
e-ISBN (PDF) 978-3-11-029225-1
e-ISBN (EPUB) 978-3-11-038887-9
Set-ISBN 978-3-11-029226-8

Library of Congress Cataloging-in-Publication Data

A CIP catalog record for this book has been applied for at the Library of Congress.

Bibliographic information published by the Deutsche Nationalbibliothek

The Deutsche Nationalbibliothek lists this publication in the Deutsche Nationalbibliografie; detailed bibliographic data are available on the Internet at <http://dnb.dnb.de>.

© 2016 Walter de Gruyter GmbH, Berlin/Boston
Cover image: gettyimages/thinkstockphotos, Abalone Shell
Typesetting: PTP-Berlin, Protago-TEX-Production GmbH, Berlin
Printing and binding: CPI books, GmbH, Leck
☉ Printed on acid-free paper
Printed in Germany

www.degruyter.com

Preface

Ceramic matrix composites (CMCs) are materials “in which one or more different ceramic phases are deliberately added, in order to increase some property that is not controlled by the monolithic ceramic materials”. The majority of CMCs contain a ceramic matrix (alumina, silicon nitride, silicon carbide, titanium carbide, and several types of glass) with metallic or ceramic fibers (short fibers such as whiskers or long fibers) or particulates as reinforcements. CMCs consist of a ceramic primary phase embedded with a secondary phase. The integration of the secondary phase into ceramic matrix results in improvement of mechanical properties, namely, its toughness. In general, CMCs are resistant to high temperatures and have good wear resistance. Also reinforcements are added during the processing of CMCs to improve the properties such as electrical conductivity, thermal conductivity, and thermal expansion.

The present volume aims to provide recent information on ceramic matrix composites – materials, manufacturing and engineering – in six chapters. Chapter 1 provides information on the mechanical behavior of ceramic matrix composite and lifetime prediction by acoustic emission. Chapter 2 is dedicated to advanced electroceramic composites (property control through processing). Chapter 3 describes the regulation and control of macro-micro structure for optimal performance in alumina self-lubricated composites. Chapter 4 contains information on the measurement of mechanical properties of interfaces in ceramic composites. Chapter 5 describes carbonaceous nanomaterials for hybrid organic photovoltaic application. Finally, Chapter 6 is dedicated to a review on advances in self-healing based on carbon nanomaterials for electrical circuits.

This book can be used as a research book for the final undergraduate engineering course or as a topic on ceramic matrix composites at the postgraduate level. Also, the book can serve as a useful reference for academics, researchers, materials, mechanical and manufacturing engineers, and professionals in ceramic matrix composites and related industries. This book is of interest for many important research centers, laboratories, and universities as well as industry. Therefore, it is hoped this book will inspire and enthuse others to undertake research in the field of ceramic matrix composites.

The editor wishes to thank De Gruyter for this opportunity and for their enthusiastic and professional support. Finally, I would like to thank all the chapter authors for participating in this work.

Aveiro, Portugal, July 2016

J. Paulo Davim

Contents

Preface — V

List of contributing authors — XI

Nathalie Godin, Pascal Reynaud, Mohamed R'Mili, and Gilbert Fantozzi

1 Mechanical behavior of ceramic matrix composite (CMCs) and lifetime prediction by acoustic emission — 1

- 1.1 Introduction — 1
- 1.2 Acoustic emission: Analysis and methodology — 3
 - 1.2.1 Location of the AE signal — 3
 - 1.2.2 Relevant descriptors — 4
 - 1.2.3 Clustering of the AE signal — 6
 - 1.2.4 Recorded AE energy vs source energy — 8
 - 1.2.5 Identification of attenuation parameters — 8
 - 1.2.6 Coefficient of emission R_{AE} — 8
 - 1.2.7 Power law — 9
- 1.3 Results during mechanical tests — 10
 - 1.3.1 Monotonic tensile behavior — 10
 - 1.3.2 Static fatigue at intermediate temperature — 14
 - 1.3.3 Cyclic fatigue at high temperature — 26
- 1.4 Conclusion — 31

Ajay Kaushal and J.M.F. Ferreira

2 Advanced electroceramic composites: Property control through processing — 39

- 2.1 Introduction — 39
- 2.2 Experimental details — 41
 - 2.2.1 Synthesis of BZT–BCT ceramics through an aqueous colloidal processing route — 41
 - 2.2.2 Structural characterization of sintered BZT–BCT ceramic samples — 42
 - 2.2.3 Mechanical characterization of sintered BZT–BCT ceramic samples — 43
 - 2.2.4 Electrical characterization of sintered BZT–BCT ceramic samples — 43
- 2.3 Results and discussion — 43
 - 2.3.1 Structural properties — 43
 - 2.3.2 Mechanical properties — 49
 - 2.3.3 Electrical properties — 51
- 2.4 Conclusions — 56

Yongsheng Zhang, Junjie Song, Yuan Fang, Hengzhong Fan, and Litian Hu

3 Regulation and control of macro-micro structure for optimal performance in alumina self-lubricated composites — 59

- 3.1 Introduction — 59
- 3.2 Influence of structure parameters on the mechanical properties of the alumina-laminated composites — 60
- 3.3 Influence of structure parameters on the tribological properties of the alumina laminated composites — 65
- 3.4 Design of interfaces for the optimal performance of laminated composites — 69

Dariusz M. Jarzabek and Wojciech Dera

4 The measurement of mechanical properties of interfaces in ceramic composites — 77

- 4.1 Introduction — 77
 - 4.1.1 The role of the interface — 77
 - 4.1.2 The basics of fracture theory — 78
- 4.2 The nanoindentation techniques — 81
 - 4.2.1 Short introduction to nanoindentation — 81
 - 4.2.2 Pushing out a fiber — 82
 - 4.2.3 Indentation tests of thin films — 83
 - 4.2.4 Compression of micropillar test specimen — 86
 - 4.2.5 Conclusion — 87
- 4.3 Pull-out and microbond tests — 88
- 4.4 Tensile tests — 90
 - 4.4.1 Interfacial shear strength measurement — 90
 - 4.4.2 Interfacial tensile strength measurement — 91
- 4.5 Scratch test — 96
 - 4.5.1 Conventional scratch test — 96
 - 4.5.2 The precracked line scratch test — 97
 - 4.5.3 Microdot scratch test — 97
- 4.6 Application of scanning force microscope in the interface strength determination — 99
 - 4.6.1 Short introduction to atomic force microscopy — 99
 - 4.6.2 Interface strength determination with nanopillars — 101
- 4.7 Concluding Remarks — 104

Brahim Aïssa and Mohammed Bououdina

5 Carbonaceous nanomaterials for hybrid organic photovoltaic application — 109

- 5.1 Introduction — 109
- 5.2 Carbon nanotubes in photovoltaic — 111

- 5.3 Graphene in photovoltaics — **116**
- 5.4 Carbon nanotubes/graphene hybrid for solar cell application — **120**
- 5.5 Outlook and perspectives — **121**

Brahim Aïssa

- 6 Advances in self-healing based on carbon nanomaterials for electrical circuits – A review — 127**
 - 6.1 Introduction — **127**
 - 6.2 State of the art — **127**
 - 6.3 Conclusions — **140**

List of contributing authors

Chapter 1

Nathalie Godin

INSA de Lyon
MATEIS (UMR CNRS 5510)
7 avenue Jean Capelle
69621 VILLEURBANNE Cedex
France
e-mail: nathalie.godin@insa-lyon.fr

Pascal Reynaud

INSA de Lyon
MATEIS (UMR CNRS 5510)
7 avenue Jean Capelle
69621 VILLEURBANNE Cedex
France

Mohamed R'Mili

INSA de Lyon
MATEIS (UMR CNRS 5510)
7 avenue Jean Capelle
69621 VILLEURBANNE Cedex
France

Gilbert Fantozzi

INSA de Lyon
MATEIS (UMR CNRS 5510)
7 avenue Jean Capelle
69621 VILLEURBANNE Cedex
France

Chapter 2

Ajay Kaushal

Department of Materials and Ceramic
Engineering, CICECO
University of Aveiro
3810-193 Aveiro
Portugal
e-mail: Ajay.kaushal@ua.pt

J.M.F. Ferreira

Department of Materials and Ceramic
Engineering, CICECO
University of Aveiro
3810-193 Aveiro
Portugal
e-mail: jmf@ua.pt

Chapter 3

Yongsheng Zhang

State Key Laboratory of Solid Lubrication
Lanzhou Institute of Chemical Physics
Chinese Academy of Science
Lanzhou 730000
China
e-mail: zhysh@licp.cas.cn

Junjie Song

State Key Laboratory of Solid Lubrication
Lanzhou Institute of Chemical Physics
Chinese Academy of Science
Lanzhou 730000
China
University of Chinese Academy of Sciences
Beijing 100049
China

Yuan Fang

State Key Laboratory of Solid Lubrication
Lanzhou Institute of Chemical Physics
Chinese Academy of Science
Lanzhou 730000
China
University of Chinese Academy of Sciences
Beijing 100049
China

Hengzhong Fan

State Key Laboratory of Solid Lubrication
Lanzhou Institute of Chemical Physics
Chinese Academy of Science
Lanzhou 730000
China
University of Chinese Academy of Sciences
Beijing 100049
China

Litian Hu

State Key Laboratory of Solid Lubrication
Lanzhou Institute of Chemical Physics
Chinese Academy of Science
Lanzhou 730000
China

Chapter 4

Dariusz M. Jarzabek

Institute of Fundamental Technological Research
Polish Academy of Sciences
Poland
e-mail: djarz@ippt.pan.pl

Wojciech Dera

Institute of Fundamental Technological Research
Polish Academy of Sciences
Poland

Chapter 5

Brahim Aïssa

Qatar Environment & Energy Research Institute
(QEERI)
and
College of Science and Engineering
Hamad Bin Khalifa University
Qatar Foundation
P.O. Box 5825
Doha, Qatar
e-mail: baissa@qf.org.qa

Mohammed Bououdina

Department of Physics
Coolege of Science
University of Bahrain
P.O. Box 32038
Sakheer Campus
Kingdom of Bahrain
e-mail: mboudina@gmail.com

Chapter 6

Brahim Aïssa

Qatar Environment & Energy Research Institute
(QEERI)
and
College of Science and Engineering
Hamad Bin Khalifa University
Qatar Foundation
P.O. Box 5825
Doha, Qatar
e-mail: baissa@qf.org.qa

Yongsheng Zhang, Junjie Song, Yuan Fang, Hengzhong Fan, and Litian Hu

3 Regulation and control of macro-micro structure for optimal performance in alumina self-lubricated composites

3.1 Introduction

High-performance alumina-matrix composites are potential candidates for the application of wear-resistance components, due to their high wearability and hardness, low specific density, corrosion resistance, and antioxidation. Nevertheless, the lubricating problems and brittleness of these structural materials are major constraints to promoting them for practical application. Therefore, it is significant to design and fabricate alumina-matrix composites with excellent mechanical and tribological properties.

The combination of the bionic design of ceramic materials and self-lubricating ceramic-matrix composites with excellent lubricating properties is a promising way to achieve the optimal integration of mechanical and tribological properties [1–3]. During the past decade, laminated ceramic composites with weak layers which inspired from bionic multilayer structures like shells, due to their excellent mechanical properties, have attracted many researchers. Based on the layered structure design concept, Clegg et al. [4] used SiC as strong layers and graphite as the weak interface successfully fabricated the SiC/graphite laminated composites, which exhibited great mechanical properties, with the fracture toughness and work of fracture being $15 \text{ MPa m}^{1/2}$ and $4,625 \text{ J m}^{-2}$, respectively. Moreover, the laminated composites also have excellent lubricating properties and wear resistance because of their special weak interfacial layer [5, 6]. According to previous studies, $\text{Al}_2\text{O}_3/\text{Mo}$ composites with a laminated structure have excellent self-lubricating and mechanical properties [6]. The existence of the weak interfacial layer of Mo results in high fracture toughness and low friction coefficient. The fracture toughness of the prepared materials could be 1.6 times higher than that of monolithic Al_2O_3 ceramics. In addition, their friction coefficient could be reduced to 0.34 when subjected to dry sliding wear against Al_2O_3 pins at 800°C under a load of 70 N with sliding frequency of 2 Hz, a decrease of approximately 60% below the monolithic Al_2O_3 ceramics.

Compared to traditional monolithic ceramics, the laminated self-lubricating composites have many advantages resulting from the laminated structure and lubricants. It is perceivable that for laminated composites with weak layers, structural parameters and interfacial characteristics have enormous effects on both their mechanical and tribological properties. The geometric parameters of the layered structure and interfacial characteristics are the key factors for the optimal design of materials with the same compositions [7–13]. Previous studies showed that the structural parameters

significantly affect the performance of laminates. The strength and fracture toughness of the materials were not only depended on the thickness of Al_2O_3 and weak layers, but also on the thickness ratio of strong-weak layers. With the increase in the layer thickness ratio, the bending strength of $\text{Al}_2\text{O}_3/\text{W}$ laminates also increases, but the fracture toughness decreases [10]. In order to obtain the maximum toughening effect, the thickness of the strong layers and weak layers as well as the thickness ratio must be kept at an appropriate value. In addition, the interfacial characteristics also have an important impact on the performance of laminated composites. It is an effective method to optimize the properties of the laminated composites through implanting special interface with controllable morphology or adjusting the compositions of weak layers [7, 11, 12]. Any modification of the interface will be a determining factor in the strength of the interfacial bond and thereby affect the crack propagating path, interfacial residual stress, and interfacial fracture resistance of laminated composites. Moreover, these interfacial designs may ensure the reliability of these materials in practical application. Therefore, it is an effective method to improve the properties of laminated composites by adjusting the structure parameters and interfacial characteristics.

Based on the above background, two kinds of ceramic composites with high reliability were designed and prepared which can achieve stable and effective lubrication at room- and high-temperature conditions, respectively. The relation between the macro-micro structure of the prepared materials and their properties was investigated.

3.2 Influence of structure parameters on the mechanical properties of the alumina-laminated composites

For laminated composites with a weak layer, the geometrical parameters of the layered structure are the key factors for the optimal design of the multilayer materials. The structural parameters mainly include the number and thickness of the matrix layers and the weak layers. In order to investigate in depth the effect factors on the mechanical properties of the materials, a series of $\text{Al}_2\text{O}_3/\text{Mo}$ and $\text{Al}_2\text{O}_3/\text{graphite}$ laminated self-lubricating composites with different structure parameters were prepared through layer-by-layer method and hot-pressing process [14, 15]. Figure 3.1 illustrates the schematic and the design concept of laminated composites. The thickness of the A layer and B layer are d_1 and d_2 , respectively, where the A layer is the Al_2O_3 and the B layer is Mo or graphite.

The microstructures of typical $\text{Al}_2\text{O}_3/\text{Mo}$ and $\text{Al}_2\text{O}_3/\text{graphite}$ laminated materials are given in Fig. 3.2 [14, 15], where the dark layer is the Al_2O_3 layer and the light layer is the Mo or graphite layer that is markedly thinner than the Al_2O_3 layer. The laminated composites presents an obvious multilayer structure, and a relatively straight weak interface can be observed without clear delamination, and the boundary between the strong layer and weak layer is sharp. Moreover, the graphite layers in the compos-

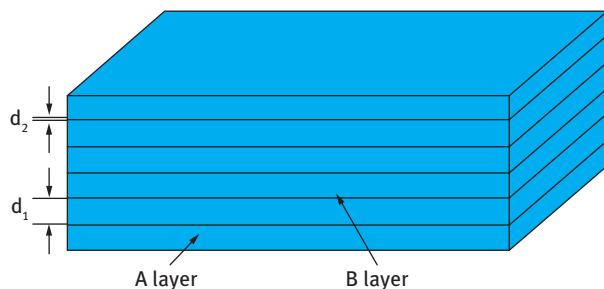


Fig. 3.1: The schematic and design concept of laminated composites.

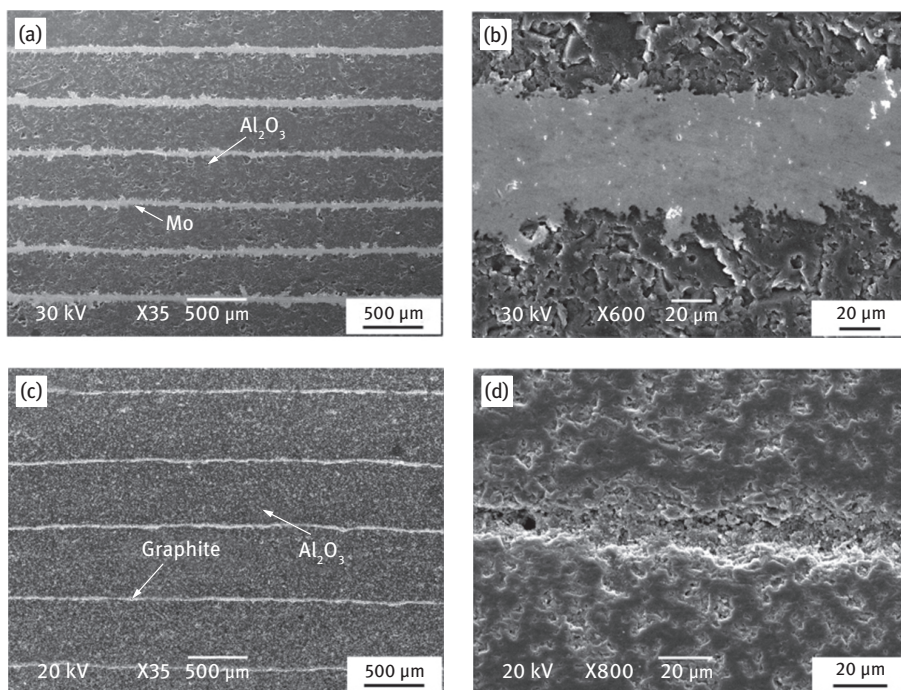


Fig. 3.2: Microstructure of the $\text{Al}_2\text{O}_3/\text{Mo}$ (a and b) and $\text{Al}_2\text{O}_3/\text{graphite}$ (c and d) laminated composites.

ites are not fully densified, due to its poor sinterability, while the metal Mo and Al_2O_3 present compact crystallized structures and have no obvious flaws. These special weak interfacial layers play an important role in improving the mechanical and tribological properties of the laminated composites.

Figure 3.3 summarizes the influence of structural parameters on the toughness and work of fracture of $\text{Al}_2\text{O}_3/\text{Mo}$ and $\text{Al}_2\text{O}_3/\text{graphite}$ laminated composites and monolithic Al_2O_3 ceramics. When the number of Al_2O_3 layers was 15 and Mo layers

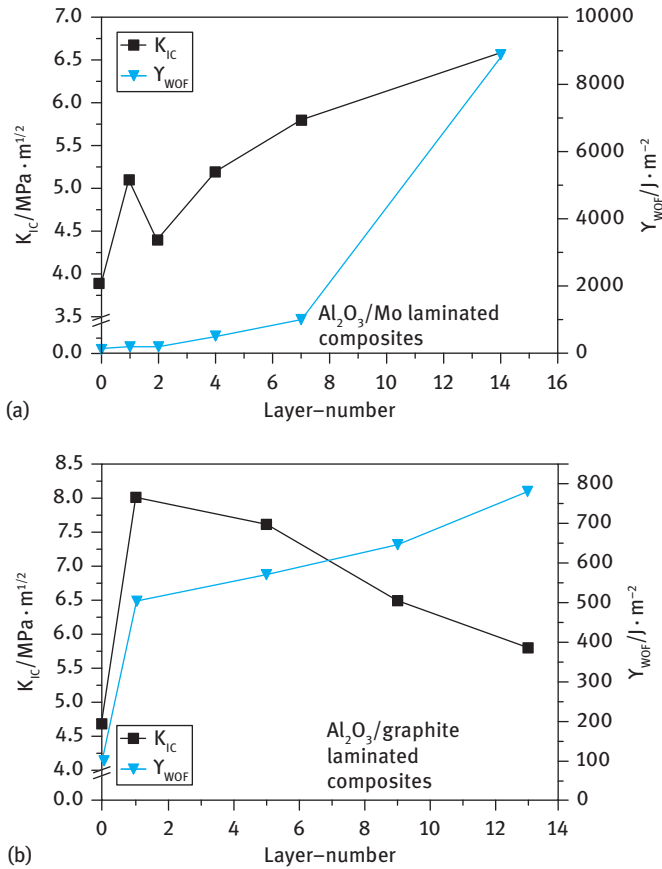


Fig. 3.3: Effect of the numbers of weak layers on the mechanical properties of the laminated composites.

14, the toughness and work of fracture of Al₂O₃/Mo laminated composites could reach 6.6 MPa m^{1/2} and 8757 J m⁻², respectively, which were 1.7 and 58.4 times higher than those of monolithic Al₂O₃ ceramics. Meanwhile, when the number of graphite layers was 5, the Al₂O₃/graphite laminated composite showed the best comprehensive properties. The toughness and work of fracture of this kind of material could reach 7.6 MPa m^{1/2} and 572 J m⁻², which were approximately 1.6 and 5.5 times higher than those of monolithic Al₂O₃ ceramic, respectively.

Taken as a whole, the laminated composites have a better fracture toughness compared with monolithic Al₂O₃ ceramic. This is mainly because the weak layer acts as a geometrical obstacle to separate the intact Al₂O₃ layer from the crack tip, that is, intact Al₂O₃ layers have a higher resistance against crack initiation than the pre-cracked Al₂O₃ layer [16]. Therefore, a smaller effective thickness of Al₂O₃ in front of the pre-crack (d_p) is rather conducive to a higher fracture toughness, especially for

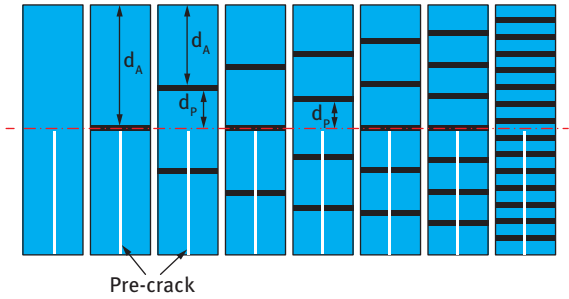


Fig. 3.4: The schematic diagram of precracked monolithic Al_2O_3 ceramic and laminated composites with different layer-numbers.

the materials having the same effective number of weak layer (n). Thus, designing the laminated composites with an even number of the ceramic layers is better for the apparent toughness of the materials (Fig. 3.4). Additionally, the effective numbers of the weak layers also have an effect on the properties of the materials. With the increase in the effective numbers of the weak layers, the work of fracture of the laminated composites increased significantly. A higher number of the weak layers will cause more dissipation of fracture energy by crack deflection, crack blunting, matrix layer pull-out, frictional bridging, and so on (Fig. 3.5). Thus, the laminated composites with a large number of weak layers show a more noncatastrophic fracture behavior, while the

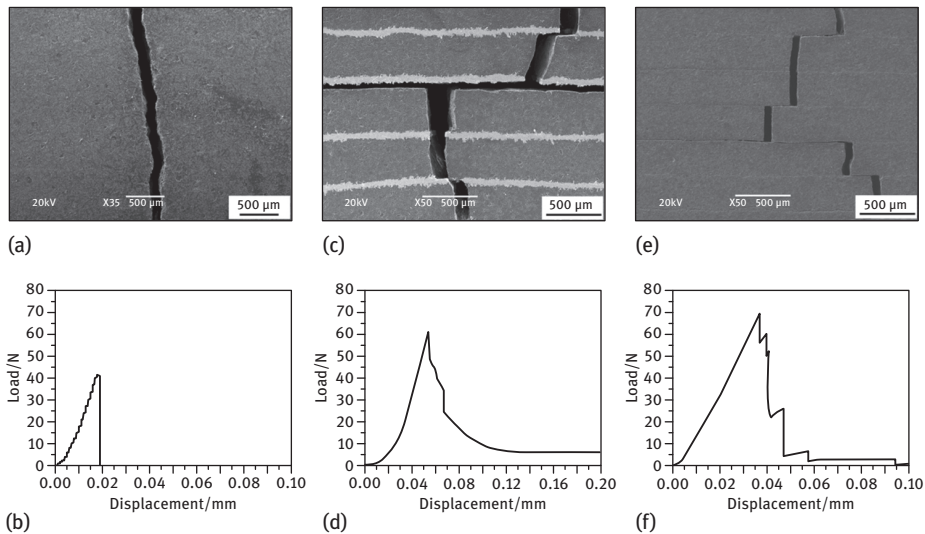


Fig. 3.5: The typical SEM images of crack propagating path and load-displacement curves of monolithic Al_2O_3 ceramic (a and b), $\text{Al}_2\text{O}_3/\text{Mo}$ (c and d) and $\text{Al}_2\text{O}_3/\text{graphite}$ (e and f) laminated composites.

materials with a small number of weak layers have a few dissipation mechanisms of fracture energy and even show brittle fracture characteristics (Fig. 3.5). Moreover, the effective number of weak layers also significantly effects the contribution of the weak layers to the toughness of the composites. For the laminated composites with ductile metal layers, the increase of the effective layer number of Mo will cause an increase of the area fraction of the ductile phase (Fig. 3.4), and thereby improve the contribution of the metal phase to the toughness of the composite. Therefore, the larger the effective number of the Mo layers is, the higher the toughness and work of fracture will be (Fig. 3.3). However, for the laminated composites with the graphite layers, the effective layer number of weak layers has a counter-effect on the toughness of materials compared with that on the $\text{Al}_2\text{O}_3/\text{Mo}$ laminated composites. Graphite is known to be material with extremely low bending strength. So the intact Al_2O_3 layers play a dominant role in the loading and fracture process. The fracture toughness is related to the value of maximum force in the process of complete rupture of the sample. The more effective number of the graphite layer (n) will cause thinning of the effective thickness of the intact Al_2O_3 layers in front of the precrack (Fig. 3.4), and thus decrease the fracture toughness of the materials. Therefore, the larger the number of graphite layers, the lower the toughness will be (Fig. 3.3). The combined action of the values of n , d_p and d_A influenced the mechanical properties of laminated composites.

In addition, the thickness of the weak layer also has a great impact on the mechanical properties of the laminated composites. Figure 3.6 summarizes the influence of the layer thickness of graphite on the toughness and work of fracture of $\text{Al}_2\text{O}_3/\text{graphite}$ laminated composites. It can be seen, with the increases of the thickness of the graphite layer, the fracture toughness of the laminated composites first increases and then gradually decreases, and the work of fracturing shows a diminishing trend. The thickness of a graphite layer that is either too small or too large is unfavorable to the improvement of fracture toughness. It is difficult to form a continuous layer of graphite if the thickness of graphite layer is too small, which is not conducive to the crack deflection (Fig. 3.7 a). If the thickness of the graphite layer is too large, the residual stress

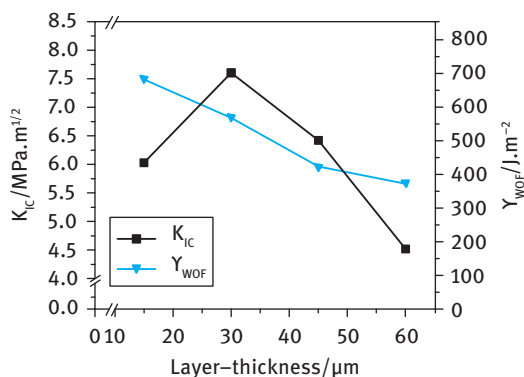


Fig. 3.6: Effect of the layer-thickness of graphite on fracture toughness and work of fracturing of the $\text{Al}_2\text{O}_3/\text{graphite}$ laminated composites.

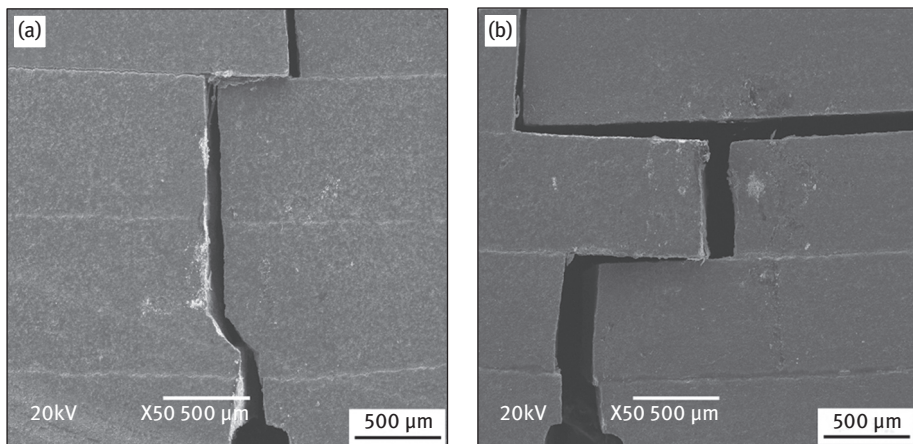


Fig. 3.7: SEM images of crack propagating path of Al_2O_3 /graphite laminated composites with a relatively thin graphite layer (a) and thick graphite layer (b).

will cause the occurrence of delamination in materials. And the frictional sliding between layers in fracture processing will become the sliding inside graphite (Fig. 3.7 b), and thereby decrease the fracture resistance [14].

Therefore, the combined contributions of the weak layer and alumina layer to the crack propagation energy and load-carrying ability of the materials influence the fracture toughness and the work of the fracture of laminated composites. The greater the effective number of the weak layers, the more the work of fracture of the materials will be. The higher the value of effective intact thickness of Al_2O_3 layers in front of the pre-crack, the better the load-carrying ability and higher fracture toughness of the materials. Consequently, the mechanical properties of the laminated composites can be flexibly optimized by the adjusting parameters of layered structure [14, 15].

3.3 Influence of structure parameters on the tribological properties of the alumina laminated composites

From the above results, the bionic layered structure design realizes the improvement of the mechanical properties for the alumina-matrix composites, and the properties of the materials were further enhanced by optimizing the structure parameters. Therefore, the layered structure and its structure parameters play an important role in the performance of the ceramic materials. To systematically investigate the effects of geometrical parameters of the layered structure on the tribological properties of the laminated composites, the relationship among the structure parameters, formation of lubricating and transferring films, load-bearing capacities and wear mechanisms were studied [5, 17].

The variations of the friction coefficients with different layer number of weak layers and layer-thickness ratio (d_1/d_2) for the $\text{Al}_2\text{O}_3/\text{Mo}$ (Figs. 3.8 a,b) and $\text{Al}_2\text{O}_3/\text{graphite}$ (Figs. 3.8 c,d) laminated composites were summarized in Fig. 3.8 [5, 17]. Compared with the monolithic Al_2O_3 ceramics, $\text{Al}_2\text{O}_3/\text{Mo}$ and $\text{Al}_2\text{O}_3/\text{graphite}$ laminated composites exhibited excellent tribological properties at 800 °C and room temperature, respectively. The optimal friction coefficient of the $\text{Al}_2\text{O}_3/\text{Mo}$ laminated composites can be reduced to 0.43 when sliding against Al_2O_3 pins at 800 °C under a load of 70 N with sliding frequency of 10 Hz. Meanwhile, the friction coefficient of the $\text{Al}_2\text{O}_3/\text{graphite}$ laminated composites can reach 0.31 when subjected to dry sliding conditions at room temperature and when coupled with Al_2O_3 balls under a load of 35 N and frequency of 5 Hz. Furthermore, it can be observed in Fig. 3.9 [5, 17] that the friction coefficient of the monolithic Al_2O_3 ceramic shows shrewd fluctuation, while that of the laminated composites are relatively steady. This is mainly attributed to the formation of the lubricating and transferring films on the sliding surfaces from lubricants or their reaction products. For the $\text{Al}_2\text{O}_3/\text{Mo}$ laminated composites at 800 °C [17] (Fig. 3.10),

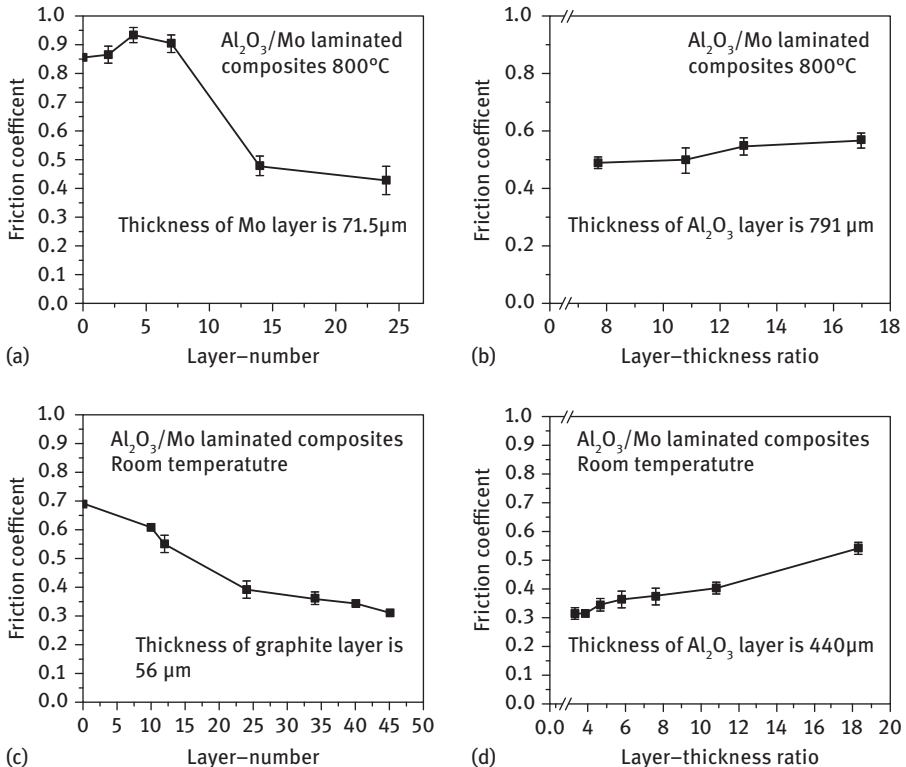


Fig. 3.8: Effect of layer-number of weak layer and layer-thickness ratio of strong-weak layers on the friction coefficient of laminated composites.

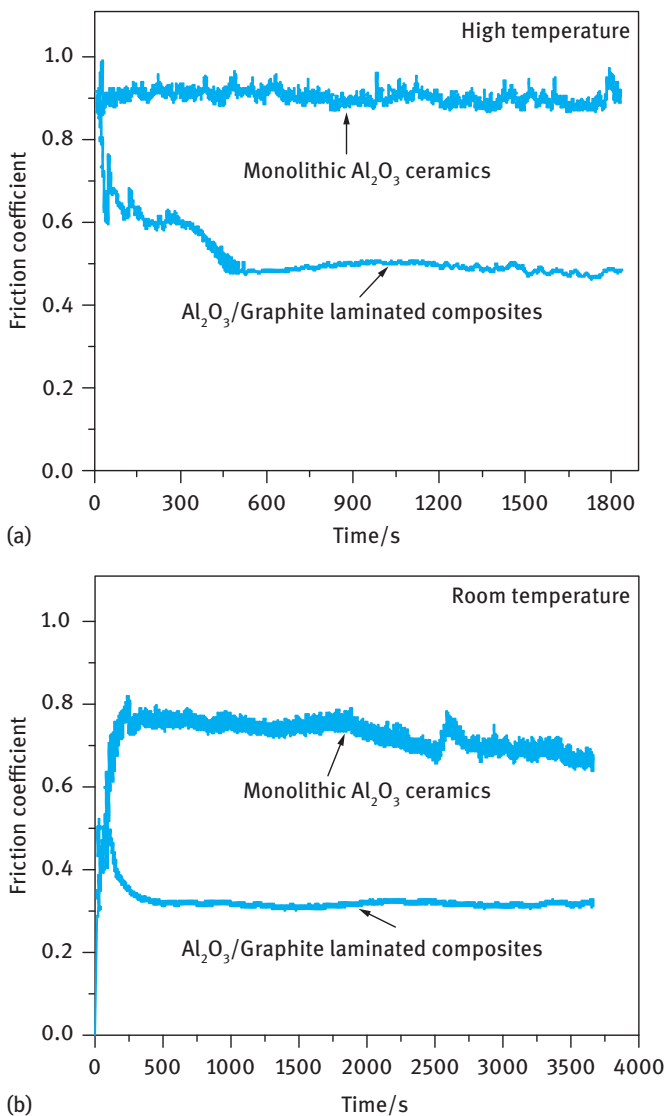


Fig. 3.9: Friction coefficient curves of monolithic Al_2O_3 ceramics, $\text{Al}_2\text{O}_3/\text{Mo}$, and Al_2O_3 /graphite laminated composites at high temperature and room temperature.

metal molybdenum exposed to the air reacts with the oxygen in the air and forms molybdenum oxide. MoO_3 has relatively low hardness and demonstrates low shear stress, which makes it easier to smear during sliding, and thereby reducing the resistance of friction [17, 19, 20]. During the friction test, the amount of molybdenum oxide increases, and they smear on the friction surface to form lubricating and transferring films. Similarly, the graphite can act as a lubricant to promote the formation

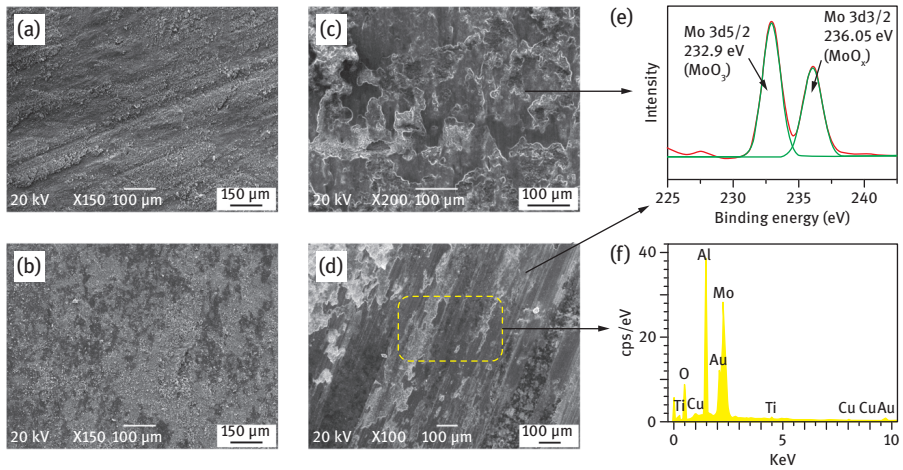


Fig. 3.10: The worn surfaces of samples and the corresponding friction pairs at 800 °C: monolithic Al_2O_3 ceramic (a, b); $\text{Al}_2\text{O}_3/\text{Mo}$ laminated composite (c–f).

of well-covered lubricating films on the surfaces of ceramics and friction pairs during dry-sliding. The formation of the well-covered lubricating and transferring films on the sliding surfaces significantly reduces the resistance of friction and also protects the ceramic and friction pair from abrasion (Fig. 3.11) [5].

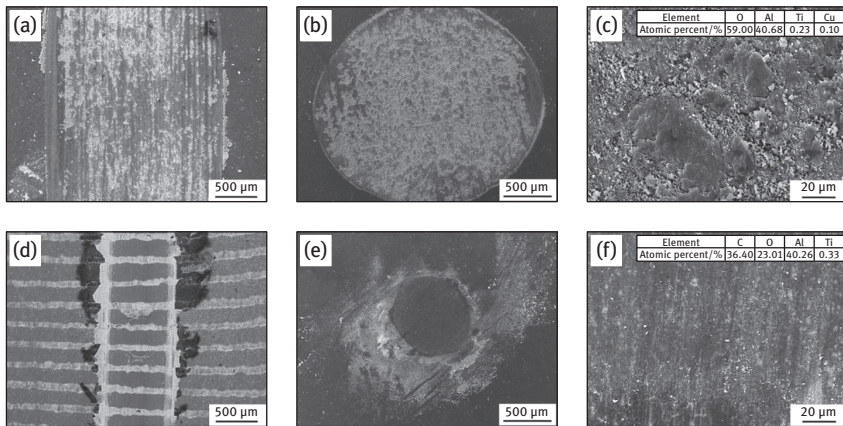


Fig. 3.11: The worn surfaces of samples and the corresponding friction pairs at room temperature: monolithic Al_2O_3 ceramic (a–c); $\text{Al}_2\text{O}_3/\text{graphite}$ laminated composite (d–f).

Moreover, the structure parameters have an enormous effect on the friction coefficient of the laminated materials. The larger the number of weak layers and smaller layer-thickness ratio (d_1/d_2), the lower will be the friction coefficient of the material. This is

mainly because the content of the lubricant phase in composites directly affects the formation of the lubricating and transferring films on the sliding surfaces. With the increase in the number of weak layers and decrease of the layer-thickness ratio (d_1/d_2), the volume fraction of the lubricant phase becomes larger, which is more conducive to the formation of successive lubricating and transferring films.

In addition, a larger layer number of weak layers and a lower layer-thickness ratio (d_1/d_2) can cause a smaller amount of space between weak layers, which is conducive to the formation of the lubricating films and the reduction of abrasion. No matter how thick the graphite layers are, the severe wear at the edge of graphite layer often occurs when the materials have a large thickness of Al_2O_3 layers (Fig. 3.12) [5]. An extremely large thickness of Al_2O_3 layers will result in a large spacing among the graphite layers, which is not better for the formation of the effective lubricating films on the friction surface during the initial stage of sliding friction, thus causing a high friction resistance. The edge of the Al_2O_3 phase near the graphite layer will be ruptured once the Al_2O_3 cannot bear the resistance of friction, followed by the accumulation of fatigue damage. Thus, a smaller spacing between the lubricant layers may be beneficial to a fewer possibilities for the rupture of ceramic at the edge of Al_2O_3 layers, especially for the graphite which has a low load-bearing capacity.

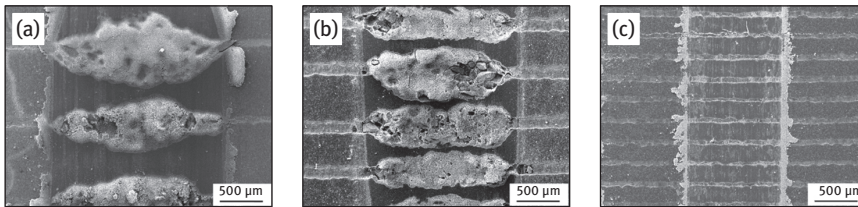


Fig. 3.12: The SEM images for the worn surfaces of Al_2O_3 /graphite laminated composites with different thickness of graphite layer and Al_2O_3 layer.

3.4 Design of interfaces for the optimal performance of laminated composites

The layered structure design and optimization of the alumina self-lubricated composites achieve the integration of the structure and lubricating function. The optimized $\text{Al}_2\text{O}_3/\text{Mo}$ and Al_2O_3 /graphite laminated composites show better lubricating properties and wear resistance than traditional monolithic self-lubricating ceramics. Considering the practical significance, the interface of materials has become an important field of research in both science and technology. For laminated composites with weak layers, interfacial characteristics may have an important effect on their mechanical and tribological properties. The interface characteristics are mainly interface chemistry and morphology. Chen et al. [11] designed and prepared layered

$\text{Al}_2\text{O}_3/\text{Ni}$ composites. They found that the toughness and strength of materials could be controlled by the tortuosity interface, which is achieved by changing the nickel layer profile. The interfacial bonding strength can be easily adjusted by this interfacial design. The mechanical interlock at the interface greatly affects the debonding length to free some of the constraint in the metal layer from the ceramic layers with applied loading and plastic deformation of the metal layer, which contributes to energy absorption [12]. Furthermore, the residual stresses vary with the change in the interface geometry [21], influencing the position of crack initiation and energy absorption through crack propagation [22]. Moreover, Wang et al. [7] indicated that adding a ceramic-matrix phase as weak interfacial layer modifier could enhance the physical strength of weak layers and the bonding strength between layers, and thereby improve the performance of the laminates. Therefore, it is an effective method to improve mechanical and tribological properties of laminated composites by implanting special interface morphologies or adjusting the compositions of weak interfaces.

To improve the overall performance of laminated composites, the $\text{Al}_2\text{O}_3/\text{Mo}$ and $\text{Al}_2\text{O}_3/\text{graphite}$ laminated composites with special interface morphology were design and prepared [14, 18]. Figure 3.13 shows the schematic and design concept of laminated composites with the controllable morphology [14, 18]. Firstly, the $\text{Al}_2\text{O}_3/\text{Mo}$ laminated composites with different interfacial texture were successfully fabricated

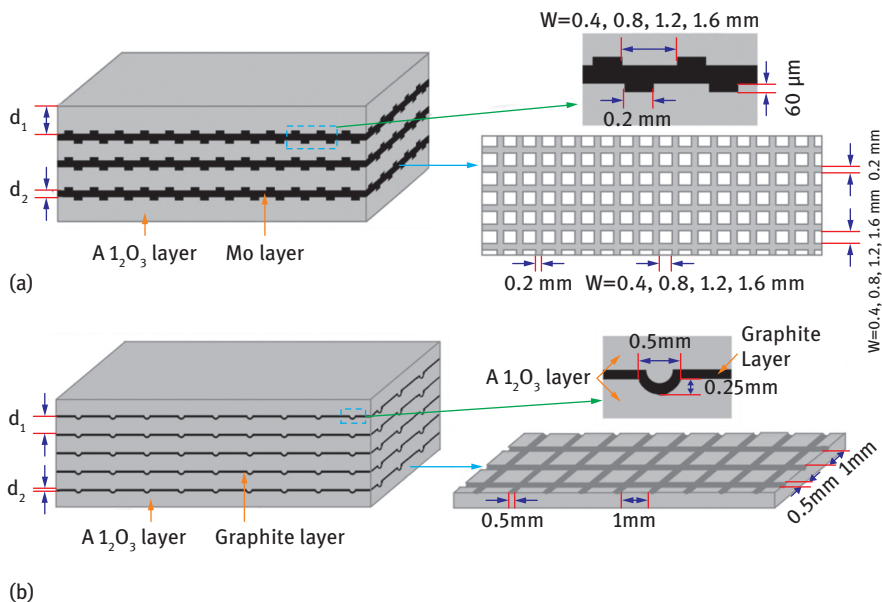


Fig. 3.13: The schematic diagram of the laminated composites: (a) the green body structure of the $\text{Al}_2\text{O}_3/\text{Mo}$ laminated composites with interfacial texture, and (b) the green body structure of the $\text{Al}_2\text{O}_3/\text{graphite}$ laminated composites with orthogonally microcorrugated interface.

(Fig. 3.13 a). The micro-textures of different densities were produced by a solid-state pulse Nd:YAG laser on the surface of an Al_2O_3 green body (Fig. 3.14 a). The grooves on the surface of the textured Al_2O_3 layers are clear and uniform, and the plateau around the grooves remains smooth (Fig. 3.14 b). The interface morphology remains clearly visible after sintering (Fig. 3.15 a), and the interfacial characteristics not only increase the contact area between the two layers but also use the mechanical interlock effectively (Fig. 3.15 b) [18].

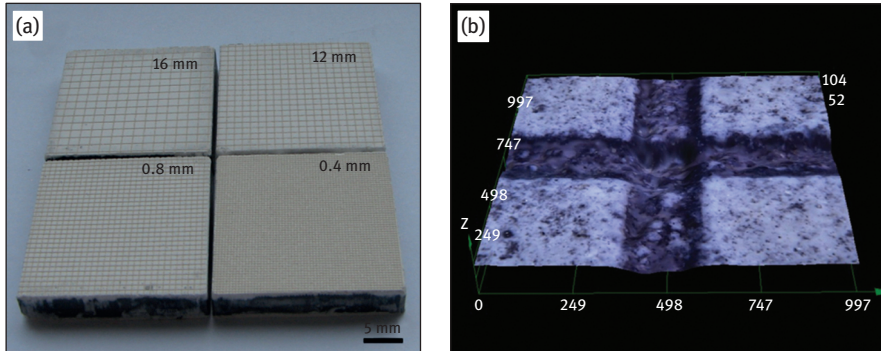


Fig. 3.14: The interfacial and profile microstructures of the $\text{Al}_2\text{O}_3/\text{Mo}$ laminated composites: (a) macroscopic features of four kinds of textured Al_2O_3 layers; (b) microstructure of textured interface.

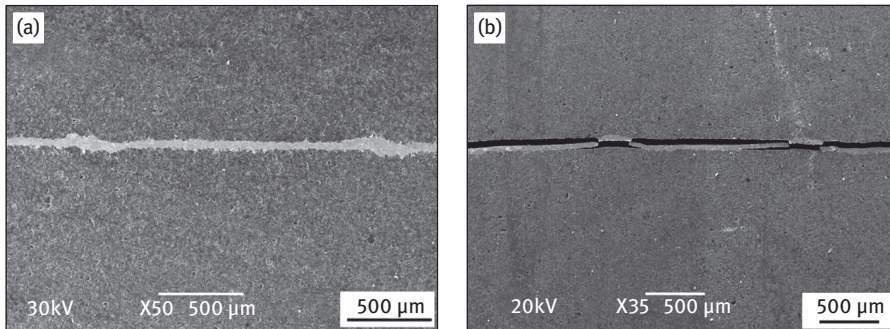


Fig. 3.15: SEM images of microstructure and the crack-path in double-shearing for the $\text{Al}_2\text{O}_3/\text{Mo}$ laminated composites with interfacial texture.

The interfacial bonding strength of the $\text{Al}_2\text{O}_3/\text{Mo}/\text{Al}_2\text{O}_3$ sandwich composites with different interfacial texture is summarized in Fig. 3.16 a. With the increase in the area density of the grooves at the interface of the Al_2O_3 layer, the interfacial bonding strength also improves linearly. The results show that the higher the area density of the grooves is, the stronger the interfacial bonding will be. The interfacial bonding

strength can be easily adjusted by this interface morphology design, confirming the previous prediction.

Moreover, this controllable interfacial morphology has a great impact on the mechanical properties of the laminated composites. Figure 3.16 [18] summarizes the influence of interfacial characteristics on the bending strength, toughness, and work of fracture of $\text{Al}_2\text{O}_3/\text{Mo}/\text{Al}_2\text{O}_3$ sandwich composites. The hot-pressed $\text{Al}_2\text{O}_3/\text{Mo}/\text{Al}_2\text{O}_3$ sandwich composites with interfacial texture exhibit excellent mechanical properties compared with the monolithic Al_2O_3 ceramics. Interfacial bonding strength that is either too strong or too weak is unfavorable for the improvement of mechanical properties. As shown in Fig. 3.15 b, the interfacial bonding strength and interfacial morphology can suppress slipping between the layers and adjust the residual stress between layers which is caused by the mismatch of the thermal expansion of the Al_2O_3 and Mo layers. If the interface bonding strength is too strong, the laminated materials will behave like a brittle monolithic ceramic, which results in low fracture toughness and work of fracture. However, if the interfacial bonding strength is too weak, less frac-

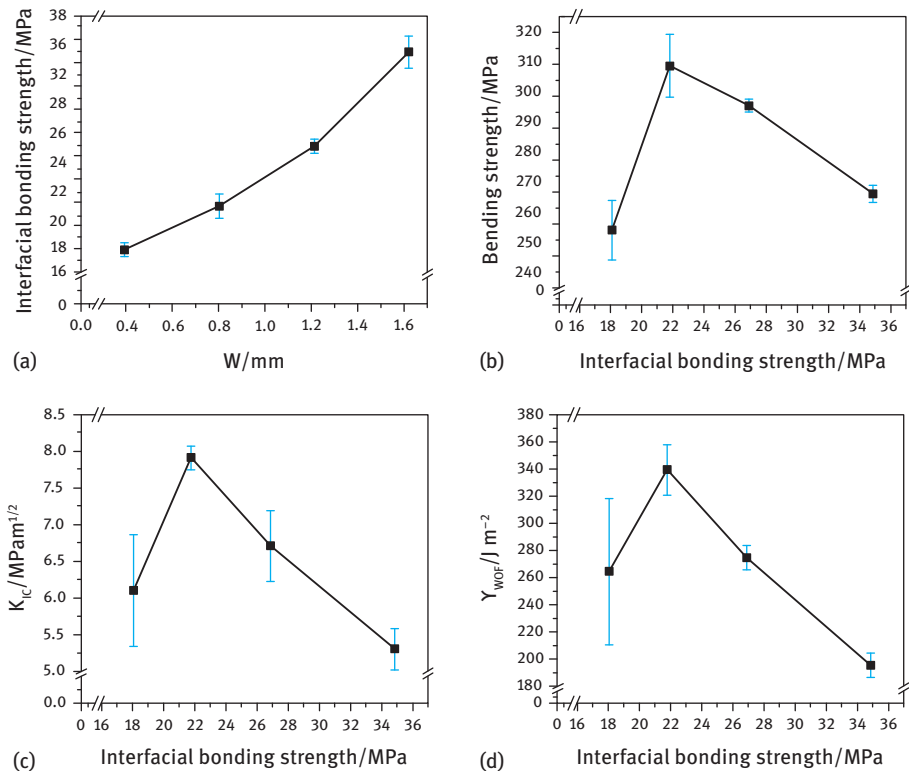


Fig. 3.16: Relationships between the area density of the interfacial texture, interfacial bonding strength, bending strength, toughness, and work of fracture of the $\text{Al}_2\text{O}_3/\text{Mo}$ composites.

ture energy will be dissipated by the resistance of special interfacial structure, which goes against the toughening of the ceramics. Meanwhile, a weaker interfacial bonding strength will also result in lower residual compressive stress of the internal layer due to lower creep constraint. Lower residual compressive stress causes a lower apparent toughness. Therefore, the combined actions of the interfacial bonding strength, interfacial morphology, and residual stress between layers influence the mechanical properties of laminated composites. Also, the performance of the composites can be easily adjusted by this interfacial design.

The toughness, bending strength, and work of fracture of $\text{Al}_2\text{O}_3/\text{Mo}/\text{Al}_2\text{O}_3$ sandwich composites can reach $79 \text{ MPa} \cdot \text{m}^{1/2}$, 309 MPa , and $339 \text{ J} \cdot \text{m}^{-2}$ when the area density of the interfacial texture is 26.5%, which is approximately 102.6%, 23.4%, and 88.83% higher, respectively, than those of monolithic Al_2O_3 ceramics [18].

Additionally, the Al_2O_3 /graphite laminated composites with orthogonally microcorrugated interface were also designed and prepared (Fig. 3.13 b) [14]. And the microcorrugated structure on the surface of the Al_2O_3 green layer is formed with a template defining a pattern having corrugated features. From Fig. 3.17, we observed that

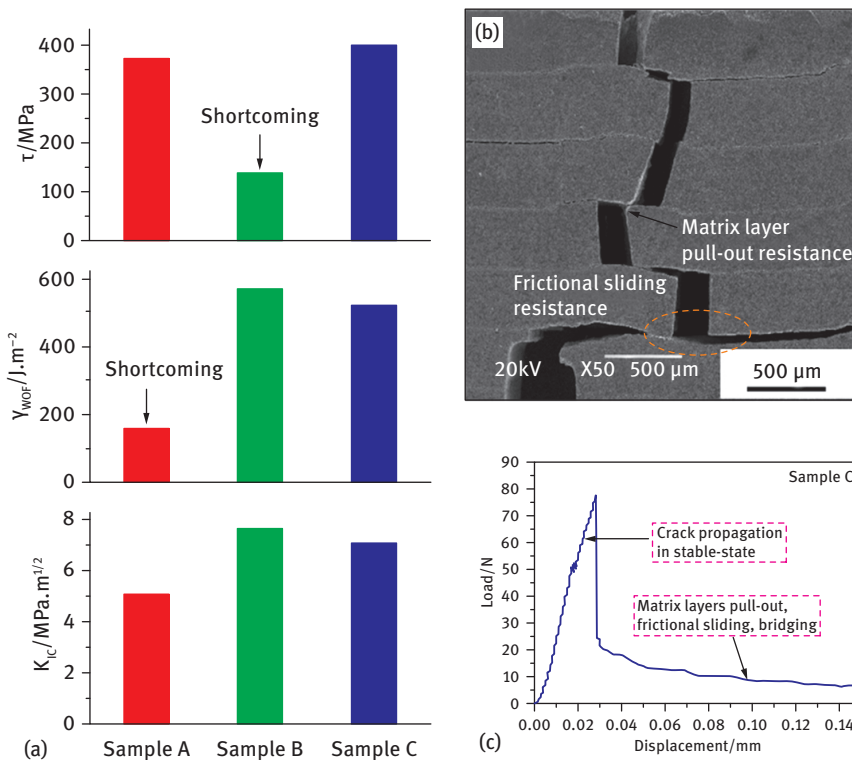


Fig. 3.17: Mechanical properties and fracture behaviors of the Al_2O_3 /graphite laminated composites with orthogonally corrugated interface.

the overall performance of the materials can be significantly improved by optimizing the design of the microinterface. This is mainly because the existing corrugated interface not only improves the crack length because of the waved weak layer, but also increases the resistance of frictional sliding. Moreover, this corrugated interfacial morphology increases the resistance in the pull-out process of the fractured matrix layer (Figs. 3.17 b,c), could significantly enhance the constraint among layers and disperse the local interfacial stresses, and thereby improve the resistance to the elastic deformation, thus increasing the bending strength of the laminated composites. Therefore, this interfacial design overcomes the delamination failure that existed in laminated composites with smooth interfaces due to the larger interface area and constraint between layers, and it also ensures the reliability of these materials in applications.

Adjusting the compositions of the interfacial layer is also a promising way to improve the overall performance of the laminated composites. Our results showed that the performance of the $\text{Al}_2\text{O}_3/\text{Mo}$ laminated composites can be further improved by introducing a transition interface with appropriate Mo content (Figs. 3.18 a,b) [15]. The fracture toughness of the materials can reach $7.3 \text{ MPa m}^{1/2}$ when the chemical component of transition interface is 50 wt.% Al_2O_3 –50 wt.% Mo. A relatively high Mo content

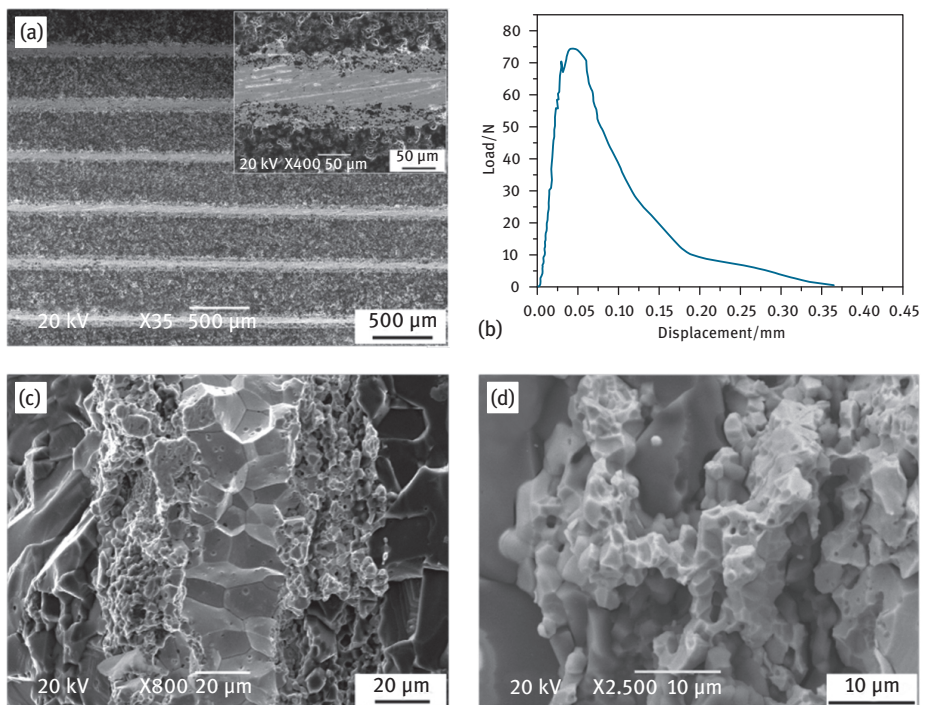


Fig. 3.18: The interfacial microstructures (a), load-displacement curve (b), and fracture surface (c) and (d) of $\text{Al}_2\text{O}_3/\text{Mo}$ laminated composites with transition interface.

in transition interfaces could improve the amount and uniformity of the interface between the two phases (Fig. 3.18 c), which is beneficial to the mechanical properties and fracture behavior of $\text{Al}_2\text{O}_3/\text{Mo}$ -laminated composites. Moreover, there exists a residual radial tensile stress and radial tangential compressive stress surrounding the Mo particles, due to the thermal expansion coefficient mismatch of the thermal expansion of ceramic particles and metal particles. Cracks will propagate in a direction parallel to the axis of the compressive stress and perpendicular to the axis of the tensile stress in the matrix (Fig. 3.18 d), which increases the extended path of the cracks and resistant force of crack expansion, and dissipates more fracture energy.

In summary, $\text{Al}_2\text{O}_3/\text{Mo}$ and $\text{Al}_2\text{O}_3/\text{graphite}$ laminated self-lubricating composites realize the integration of mechanical and lubricating properties of ceramic materials. The performance of the laminated composites can be facility controlled by the design of the structure parameters, interfacial morphology, and compositions of the weak layers. The excellent mechanical and tribological properties of the optimal laminated composites enable them to be used in a wide range of applications.

Acknowledgement

The authors acknowledge financial support from the National Natural Science Foundation of China (51575506), the Foundation for National Innovation of Chinese Academy of Sciences (CXJJ-15M059) and the Youth Innovation Promotion Association CAS (2013272).

Bibliography

- [1] Y. S. Zhang, Y. Fang, H. Z. Fan, J. J. Song, T. C. Hu, and L. T. Hu, High-performance ceramic lubricating materials, in: M. C. Wythers (ed.), *Advances in materials science research* **17**, 83–92, New York, Nova Science Publishers, 2014.
- [2] Y. Fang, Y. S. Zhang, J. J. Song, H. Z. Fan, and L. T. Hu, Design and fabrication of laminated-graded zirconia self-lubricating composites, *Mater. Des.* **49** (2013), 421–425.
- [3] Y. E. Qi, Y. S. Zhang, Y. Fang, and L. T. Hu, Design and preparation of high-performance alumina functional graded self-lubricated ceramic composites, *Compos. Pt. B-Eng.* **47** (2013), 145–149.
- [4] W. J. Clegg, K. Kendall, N. M. Alford, T. W. Button, and J. D. Birchall, A simple way to make tough ceramics, *Nature* **347** (1990), 455–457.
- [5] J. J. Song, Y. S. Zhang, Y. F. Su, Y. Fang, and L. T. Hu, Influence of structural parameters and compositions on the tribological properties of alumina/graphite laminated composites, *Wear* **338–339** (2015), 351–361.
- [6] Y. E. Qi, Y. S. Zhang, and L. T. Hu, High-temperature self-lubricated properties of $\text{Al}_2\text{O}_3/\text{Mo}$ laminated composites, *Wear* **280** (2012), 1–4.
- [7] C. A. Wang, Y. Huang, Q. F. Zan, L. H. Zou, and S. Y. Cai, Control of composition and structure in laminated silicon nitride/boron nitride composites, *J. Am. Ceram. Soc.* **85** (2002), 2457–2461.

- [8] M. E. Launey, E. Munch, D. H. Alsem, E. Saiz, A. P. Tomsia, and R. O. Ritchie, A novel biomimetic approach to the design of high-performance ceramic-metal composites. *J. R. Soc. Interface* **7** (2010), 741–753.
- [9] Q. F. Zan, C. A. Wang, Y. Huang, S. Zhao, and C. W. Li, Effect of geometrical factors on the mechanical properties of $\text{Si}_3\text{N}_4/\text{BN}$ multilayer ceramics, *Ceram. Int.* **30** (2004), 441–446.
- [10] A. Huang and C. A. Wang, Multiphase composite ceramics with high performance, 1st ed., China: Tsinghua University Press, Beijing, 2008.
- [11] Z. Chen and J. J. Mecholsky, Jr., Control of strength and toughness of ceramic/metal laminates using interface design, *J. Mater. Res.* **8**(9) (1993), 2362–2369.
- [12] Z. Chen and J. J. Mecholsky, Jr., Toughening by metallic lamina in nickel/alumina composites, *J. Am. Ceram. Soc.* **76**(5) (1993), 1258–1264.
- [13] K. H. Zuo, D. L. Jiang, Q. L. Lin, and Y. Zeng, Improving the mechanical properties of $\text{Al}_2\text{O}_3/\text{Ni}$ laminated composites by adding Ni particles in the layers, *Mat. Sci. Eng. A* **443** (2007), 296–300.
- [14] J. J. Song, Y. S. Zhang, H. Z. Fan, Y. Fang, and L. T. Hu, Design of structure parameters and corrugated interfaces for optimal mechanical properties in alumina/graphite laminated nanocomposites, *Mater. Des.* **65** (2015), 1205–1213.
- [15] J. J. Song, Y. S. Zhang, Y. Fang, H. Z. Fan, L. T. Hu, and J. M. Qu, Influence of structure parameters and transition interface on the fracture property of $\text{Al}_2\text{O}_3/\text{Mo}$ laminated composite, *J. Eur. Ceram. Soc.* **35** (2015), 1581–1591.
- [16] K. L. Hwu and B. Derby, Fracture of metal/ceramic laminates-II crack growth resistance and toughness, *Acta mater.* **47** (1999), 545–563.
- [17] Y. Fang, Y. S. Zhang, J. J. Song, H. Z. Fan, and L. T. Hu, Influence of structure parameters on the tribological properties of $\text{Al}_2\text{O}_3/\text{Mo}$ laminated nanocomposite, *Wear* **320** (2014), 152–160.
- [18] J. J. Song, Y. S. Zhang, H. Z. Fan, T. C. Hu, L. T. Hu, and J. M. Qu, Design of interfaces for optimal mechanical properties in $\text{Al}_2\text{O}_3/\text{Mo}$ laminated composite, *J. Eur. Ceram. Soc.* **35** (2015), 1123–1127.
- [19] Y. S. Zhang, L. T. Hu, J. M. Chen, and W. M. Liu, Lubrication behavior of Y-TZP/ $\text{Al}_2\text{O}_3/\text{Mo}$ nanocomposites at high temperature, *Wear* **268** (2010), 1091–1094.
- [20] Y. F. Su, Y. S. Zhang, J. J. Song, Y. Fang, and L. T. Hu, High-Temperature self-Lubricated and fracture properties of alumina/molybdenum fibrous monolithic ceramic, *Tribol. Lett.* **61** (2016), 9.
- [21] M. Ranjbar-Far, J. Absi, G. Mariaux, and F. Dubois, Simulation of the effect of material properties and interface roughness on the stress distribution in thermal barrier coatings using finite element method, *Mater. Des.* **31** (2010), 772–781.
- [22] M. Belhouari, B. B. Bouiadjra, K. Kaddouri, and T. Achour, Plasticity effect on crack growth along ceramic/metal biomaterial interface: Numerical analysis, *Mech. Adv. Mater. Struct.* **18** (2011), 364–372.